Human Molecular Genetics, 2014, Vol. 23, No. 21 **5814–5826**
doi:10.1093/hmg/ddu299
Advance Access published on June 12, 2014

Gaucher disease due to saposin C deficiency is an inherited lysosomal disease caused by rapidly degraded mutant proteins

Marialetizia Motta[1,†], Serena Camerini[2,†], Massimo Tatti[1], Marialuisa Casella[2], Paola Torreri[3], Marco Crescenzi[2], Marco Tartaglia[1] and Rosa Salvioli[1,*]

[1]Department of Haematology, Oncology and Molecular Medicine, [2]Department of Cell Biology and Neuroscience and [3]National Center for Rare Diseases, Istituto Superiore di Sanità, Viale Regina Elena 299, 00161 Rome, Italy

Received May 19, 2014; Revised and Accepted June 9, 2014

Saposin (Sap) C is an essential cofactor for the lysosomal degradation of glucosylceramide (GC) by glucosylceramidase (GCase) and its functional impairment underlies a rare variant form of Gaucher disease (GD). Sap C promotes rearrangement of lipid organization in lysosomal membranes favoring substrate accessibility to GCase. It is characterized by six invariantly conserved cysteine residues involved in three intramolecular disulfide bonds, which make the protein remarkably stable to acid environment and degradation. Five different mutations (i.e. p.C315S, p.342_348FDKMCSKdel, p.L349P, p.C382G and p.C382F) have been identified to underlie Sap C deficiency. The molecular mechanism by which these mutations affect Sap C function, however, has not been delineated in detail. Here, we characterized biochemically and functionally four of these gene lesions. We show that all Sap C mutants are efficiently produced, and exhibit lipid-binding properties, modulatory behavior on GCase activity and subcellular localization comparable with those of the wild-type protein. We then delineated the structural rearrangement of these mutants, documenting that most proteins assume diverse aberrant disulfide bridge arrangements, which result in a substantial diminished half-life, and rapid degradation via autophagy. These findings further document the paramount importance of disulfide bridges in the stability of Sap C and provide evidence that accelerated degradation of the Sap C mutants is the underlying pathogenetic mechanism of Sap C deficiency.

INTRODUCTION

Gaucher disease (GD; MIM #230800) is an inherited autosomal recessive disorder generally due to deficit of the lysosomal enzyme glucosylceramidase (GCase; MIM #606463), which in presence of its activator, saposin (Sap) C, hydrolyses glucosylceramide (GC) to glucose and ceramide (1). Deficit of GCase expression or function results in the storage of GC in lysosomes of monocyte/macrophage lineage, leading to multisystemic symptoms. GD main clinical manifestations include hepatosplenomegaly, anemia, thrombocytopenia, bone lesions and pulmonary hypertension. Based on the presence of central nervous system involvement and disease onset, GD is classified in GD1 (mild non-neuronopathic form, adult onset), GD2 (acute neuronopathic form, infantile onset) and GD3 (sub-acute neuronopathic form, juvenile or early adult onset) (1).

A rare form of GD is caused by biallelic mutations in the *prosaposin* (*PSAP*) gene (MIM #176801), which encodes the GCase activator, Sap C. This protein is a member of a family of four small glycoproteins, referred as Sap A–D, which derive from sequential lysosomal proteolysis of the precursor, PSAP. While Saps share high structural similarity and common ability to interact with membranes, their specificity and mode of action differ considerably (2,3). The pathological consequences of mutations in any one of these proteins result in clinical manifestations equivalent to those due to mutations in their cognate enzymes (4,5).

Sap C counts 80 amino acid residues, has a single *N*-glycosylation site and a structure characterized by five

*To whom correspondence should be addressed at: Department of Haematology, Oncology and Molecular Medicine, Istituto Superiore di Sanità, Viale Regina Elena 299, 00161 Rome, Italy. Tel: +39 0649902416; Fax: +39 0649387087; Email: rosa.salvioli@iss.it
†These authors equally contributed to this work.

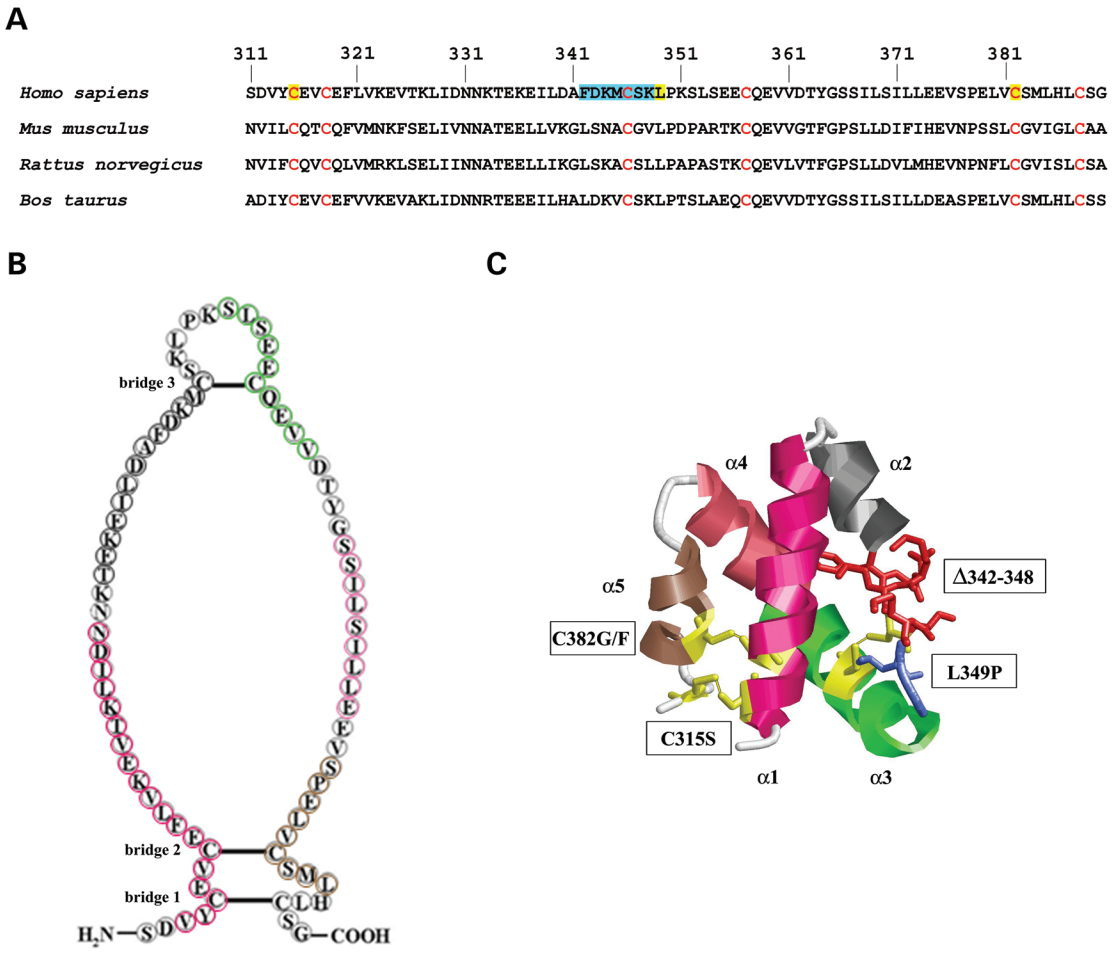

Figure 1. Sap C amino acid sequence, schematic disulfide bond structure and location of the disease-causing mutations. (**A**) Sequence alignment of the human Sap C (NP_001035931.1) with the murine (NP_035309.2), rat (NP_037145.1) and bovine (NP_776586.1) orthologs. The six conserved cysteine residues (red characters), the point mutations (yellow characters) and the deletion (azure characters) are shown. (**B**) Schematic structure of Sap C, adapted from Vaccaro *et al.* (6). Black lines linking cysteine residues indicate disulfide bonds. (**C**) Three-dimensional structure of the Sap C (PDB accession number code 2GTG) is characterized by five α-helices. Residues affected by disease-causing mutations (C315S, Δ342-348, L349P, C382G and C382F) are shown (*stick* representation).

α-helices that is stabilized by six cysteine residues, which are invariably conserved among Sap proteins (Fig. 1A) (2). These residues are involved in three intramolecular disulfide bridges: the first two cysteine residues (helix 1) are linked to the last two (helix 5) (pairings between Cys^{315} and Cys^{388}, and Cys^{318} and Cys^{382}, respectively), and the two centrally placed residues [Cys^{346} (helix 2) and Cys^{357} (helix 3)] are linked to each other (Fig. 1B) (6,7). This bonding network plays a pivotal role in stabilizing Sap C conformation, making the protein remarkably stable to heat, acid environment and proteolytic degradation (Fig. 1C) (2).

Sap C deficiency (MIM #610539) is an extremely rare disease, with five unrelated patients being reported so far (8–12). Among them, two subjects, displaying a GD3 phenotype, were heterozygous for a different amino acid change involving the same cysteine residue, c.1249G>T (p.C382F) and c.1248T>G (p.C382G) (8,9). The other mutation has been remained unidentified in one patient (13), while it was a truncating change in the second patient (14,15). Both these patients died during childhood (14 and 15.5 years, respectively). Two adult siblings were reported to be compound heterozygous for the c.1150T>C (p.L349P) and c.105A>T (p.M1L) substitutions. Both subjects displayed a GD1 phenotype (10). Two different missense mutations (c.1047T>A, p.C315S; 105A>G, p.M1V) were identified in a sporadic case exhibiting a GD3 phenotype (11). The last patient was homozygous for an in-frame deletion, c.1128_1148delT TTGACAAAATGTGCTCGAAG (p.342_348FDKMCSKdel, hereafter referred to as Δ342-348) (12). Overall, four of the five Sap C mutations described so far were documented to involve the substitution or deletion of one cysteine residue (Fig. 1C), and were predicted to break one of the three disulfide bridges.

We previously observed that the level of Sap C was dramatically reduced in primary fibroblasts of affected subjects, particularly in those carrying mutations involving a cysteine residue, while the level of PSAP was apparently unaffected (16).

Here, we explored further structural, functional and biological properties of the disease-associated C315S, Δ342-348, L349P, C382G mutants and show that lipid-binding efficiency, modulatory behavior on GCase activity and subcellular localization of these proteins are unexpectedly equivalent to those of wild-type (WT) Sap C. We demonstrate that proteins with mutations

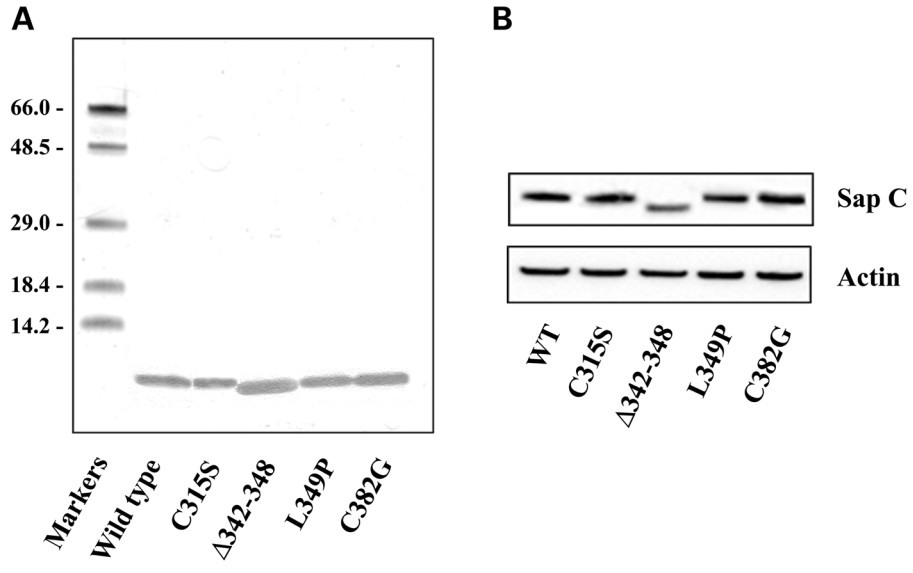

Figure 2. SDS–PAGE and western blotting of WT Sap C and disease-causing mutants. (**A**) Recombinant WT and mutant proteins (0.2 μg/lane) were visualized by silver staining. (**B**) COS-1 lysates were immunostained using an anti-V5 monoclonal antibody recognizing the tag of the expressed proteins. Actin level indicates equal loading.

involving a cysteine residue exhibit altered structural characteristics, have significantly diminished half-life and undergo accelerated degradation, leading to loss of normal Sap C function. These analyses provide further information on the hypomorphic action of the L349P mutant, which results in milder disease compared with mutations involving cysteine residue.

RESULTS

Protein expression and localization of WT and mutant Sap C proteins

To explore the molecular mechanism underlying Sap C deficiency, the biochemical and functional properties of four of the five reported disease-associated Sap C mutant proteins were analyzed. To this purpose, we generated the C315S, Δ342-348, L349P, C382G Sap C mutants and expressed them in *Escherichia coli* Origami 2 (DE3) cells (17). Electrophoretic analysis of recombinant Sap C proteins confirmed the expected molecular mass for all mutants (Fig. 2A). No product resulting from protein degradation was apparent. COS-1 cells were transiently transfected with each Sap C construct for expression and localization analysis. The WT protein and Sap C mutants (defined as immunodetectable Sap C in cell lysates) were expressed at comparable levels, with the exception of Δ342-348 that displayed a significantly reduced level (Fig. 2B). Cellular localization of all mutants was determined by indirect immunofluorescence microscopy. Each form of Sap C largely colocalized with cathepsin D (Cath D), a specific lysosomal protease, indicating that a significant proportion of proteins resided in lysosomes, similar to what observed for WT Sap C (Fig. 3).

Functional capacity of Sap C mutants

We previously reported that Sap C tightly binds to anionic phospholipid-containing membranes at low pH values, mimicking the acidic endo/lysosomal environment, and activates GCase by promoting enzyme association with lipid surface (18,19). The pH-dependent interaction of Sap C with phospholipid vesicles has been confirmed by NMR studies (7). To mimic the *in vivo* conditions, anionic phospholipid-containing liposomes were presented to a solution of WT Sap C or each one of the recombinant mutant proteins. The lipid-binding behavior of these proteins was measured using the surface plasmon resonance (SPR) spectroscopy at acidic and neutral pH values representative binding curves, obtained after injection of WT Sap C or each mutant on the immobilized large unilamellar vesicles (LUVs), are shown in Figure 4A. We observed that each protein interacted with lipid membranes at pH 5.0 (Fig. 4A, left panel). Unexpectedly, SPR measurements showed that all the mutants displayed an increased binding capacity to liposomes compared with WT Sap C, with highest lipid affinity binding for the C382G and C315S mutants. As expected, no binding to immobilized lipid bilayers was observed at pH 7.0 for all the examined Sap C proteins (Fig. 4A, right panel). Interestingly, all mutants exhibited also activating efficiency on GCase. Comparable results were obtained using either the artificial [4-methylumbelliferyl-β-glucopyranoside (4-MU-Glc)] or natural lipid substrate (GC) (Fig. 4B, left and right panel, respectively). Of note, the L349P mutant showed activation on GCase to the same extent as the WT protein, whereas the C382G mutant showed even higher activation on the enzyme.

Mass analysis of Sap C mutants

All recombinant Sap C mutants were analyzed by matrix assisted laser desorption ionization mass spectrometer (MALDI-MS) to extract information about their structure and redox state of the cysteine residues. Molecular-weight measurement of the intact proteins confirmed the presence of three disulfide bonds in L349P and WT protein, while revealed the presence of two

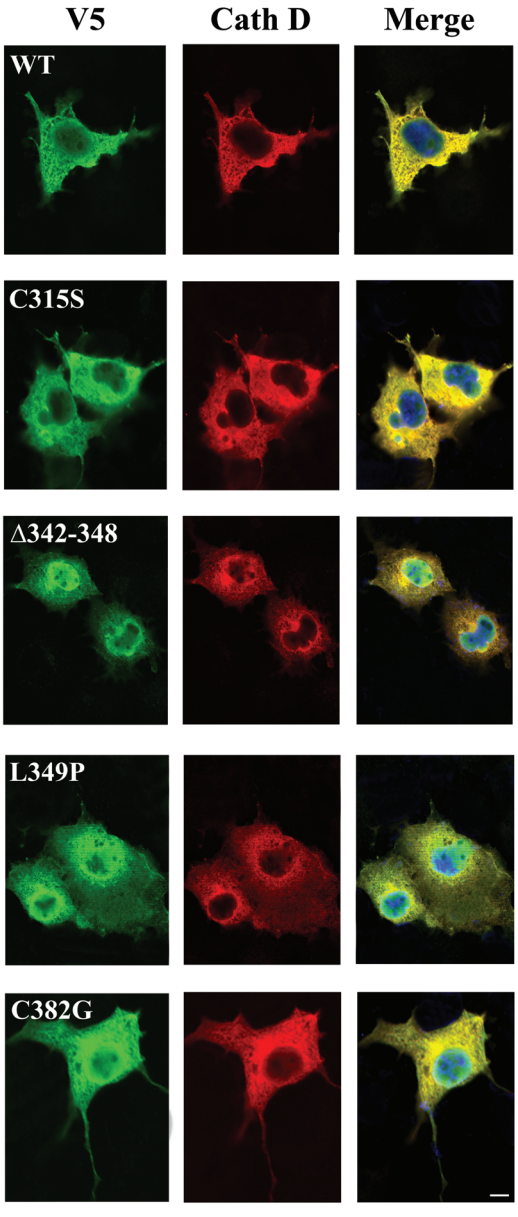

Figure 3. Localization of WT Sap C and disease-causing mutant proteins overexpressed in COS-1 cells. Cells were stained with the anti-V5 antibody (green). Co-localization analysis was performed using the lysosomal marker Cath D (red). Merged images are showed in the right panels. Scale bar, 10 μm.

disulfide bonds and one reduced cysteine in all the other mutants. This interpretation was validated by MS analysis of the proteins after iodoacetamide (IAM) alkylation: while WT and L349P proteins were unmodified by the treatment, the other three mutants showed a mass increase compatible with the addition of a single IAM molecule in agreement with the presence of one reduced cysteine (Supplementary Material, Fig. S1).

To elucidate the nature of disulfide bridges, all Sap C mutants were hydrolysed by chemical [cyanogen bromide (BrCN)] or enzymatic proteolysis. To this aim, several enzymes, alone or in combinations, were employed and the resulting peptide mixtures were analyzed by MALDI-MS. Integrating the data allowed us to deduce the complement of disulfide bonds occurring in each mutant and also the reduced cysteines. A comprehensive picture of the elucidated structures is provided by the schematic representation in Fig. 5. The L349P mutant was demonstrated to exhibit the same disulfide bridges occurring in the WT protein, indicating that substitution of Leu^{349} by proline does not influence the formation of the native 346–357 disulfide bridge. In the Δ342-348 mutant, Cys^{357}, lacking its natural-binding partner, Cys^{346}, was always detected in the alkylated form, indicating its reduced state in the mutant. The lack of amino acids 342 to 348 also affected the disulfide bonds in the *N*- and *C*-terminal regions of the protein. Indeed, even if the peaks at *m*/*z* 2493.05 and 2511.02 from Glu C digestion demonstrate the presence of the native 315–388 and 318–382 disulfide bonds, additional peaks were detected. Ions at 1719.7, 1931.7 and 1261.58 from trypsin, Asp N and Glu C digestion, respectively, reflected the existence of new disulfide bonds between cysteine residues 315–318 and 382–388. These bridges or structural rearrangement involving the *N*- and *C*-terminus of the protein are predicted to distort the native structure with possible consequences on protein stability and/or function. In the C315S and C382G mutants, the central 346–357 disulfide bond was unaffected, whereas the bridges at the termini of the proteins were variably configured. In particular, the C315S mutant was able to form either the native 318–382 or non-natural 318–388 disulfide bond. In addition, the presence of the 382–388 disulfide bridge, confined within the *C*-terminus, was detected after Glu C digestion. Similarly, both the non-natural 318–388 and the *N*-terminal 315–318 disulfide bonds were observed to occur in the C382G mutant pool.

Stability and degradation of Sap C mutants

We and others previously documented a decreased or undetectable level of Sap C in fibroblasts from patients with Sap C deficiency (8,9,16). To assess the stability of Sap C mutants, we overexpressed them in COS-1 cells and determined their half-life by treatment with the protein synthesis inhibitor cycloheximide (CHX). Western blot and relative quantitative analyses revealed a precipitous decrease in the level of Sap C mutants, being their half-life significantly reduced to 50 min (C382G), 40 min (L349P) and 20 min (C315S and Δ342-348), whereas the WT protein level was ∼67% after 1 h of treatment (Fig. 6A).

Proteins are in continuous state of flux between synthesis and degradation. Given the lysosomal localization of WT and mutant Sap C, we examined the stability of these proteins treating transfected COS-1 cells with 3-methyladenine (3-MA), an inhibitor of autophagy. We observed that all mutant proteins displayed a variable increased instability (Fig. 6B), supporting their efficient synthesis and physiologic accelerated degradation via autophagy. Consistent with this observation, no significant difference was observed in transfected cells treated with MG132 (Fig. 6C), indicating equal clearance via the ubiquitin proteasome system of aberrantly targeted proteins in cells.

Sap C mutants are prone to Cath D-mediated proteolysis

Sap C is a stable protein, able to withstand even in very high temperatures (2). Given its lysosomal localization, it also exhibits a particular resistance to the proteolytic action of proteases. Remarkably, we observed that resistance to proteolytic activity

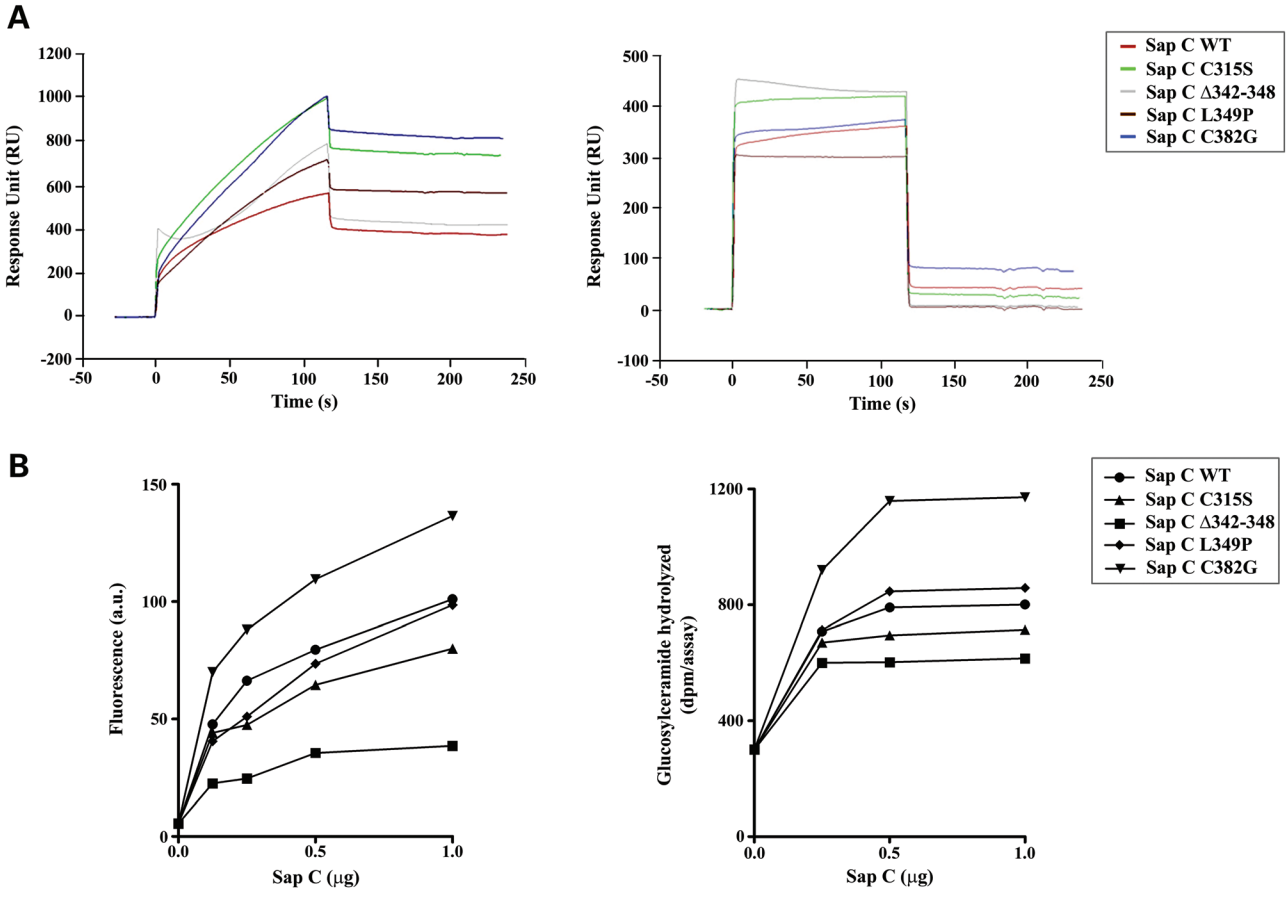

Figure 4. Interaction with immobilized vesicles and relative effect on GCase catalytic activity of WT Sap C and disease-causing mutants. (**A**) Negatively charged LUVs composed of PC and PS (80 : 20 molar ratio) were immobilized on the L1 sensor chip surface. WT Sap C and mutants (1 μM) were injected under acidic (10 mM sodium acetate, 150 mM NaCl, 1 mM EDTA and pH 5.0) (left panel) or neutral (10 mM *N*-2-hydroxyethylpiperizine-*N*-2-ethanesulphonic acid, 150 mM NaCl, 1 mM EDTA and pH 7.0) (right panel) conditions, at flow rate of 30 μl/min for 120 s during the association phase. This was followed by the injection of protein-free buffer (dissociation phase). (**B**) Increasing amounts of WT Sap C and each mutant were added to purified human GCase (4 ng) in the presence of PC:PS-containing LUVs (100 μg) and 4-MU-Glc at pH 5.0 (left panel), or in the presence of PC:PS:[^{3}H]GC-containing LUVs at pH 5.0 (right panel). Each value represents mean of at least three independent experiments.

was significantly reduced in all the mutants. This observation, along with the different stability of the proteins overexpressed in COS-1 cells, led us to investigate the role played by the different disulfide bonds on Sap C susceptibility to the proteolytic activity of lysosomal enzyme Cath D (20). After incubation with this protease for short or long times, Sap C digestion products were analyzed by MALDI-MS. The incubations were performed in the presence or absence of insulin, to ascertain Cath D activity efficiency. First, we analyzed the profiles of WT Sap C and insulin intact forms and their relative structure (Fig. 7A). Differently from what observed for insulin, which was almost completely digested by overnight (O/N) treatment, WT Sap C protein remained unaffected (Fig. 7B). The L349P mutant showed a similar behavior, since most of the protein remained intact after O/N incubation (Fig. 7C). This finding was suggestive of a slightly increased susceptibility of this mutant, which contains the point mutation localized in the central part of the protein. Cath D showed a completely different course of action on the Δ342-348 mutant, which underwent extensive digestion after 2 h, and was almost completely digested O/N. The major digestion product contained the native disulfide bridges connecting the *N*- and *C*-termini and remained intact even after an O/N digestion [peak at *m/z* 5636.50, corresponding to the (309–339) and (366–384) peptides, held together by disulfide bonds] (Fig. 7D). Similarly, the C315S mutant displayed substantial sensitivity to Cath D, several digestion products were detected already after 2 h and represented the most abundant ions after O/N treatments, when only a small fraction of the protein remained undigested (Fig. 7E). The structure containing the native Cys^{318}–Cys^{382} and Cys^{346}–Cys^{357} disulfide bonds was the most resistant species observed to be present. Digestion apparently involved the *C*-terminal region (residues 388–391), which contains the reduced Cys^{388}. The structure containing the Cys^{382}–Cys^{388} disulfide bond, confined in the *C*-terminus, was also easily digested, producing the (373–391) peptide detected at *m/z* 2046.29 and other peptides coming from the central part of the protein (Fig. 7E). Finally, the C382G mutant was partially digested by Cath D after 2 h and completely after an O/N incubation (Fig. 7F).

To provide quantitative information on the differential Cath D susceptibility of mutants, WT Sap C and each mutant were

Mutant	*Treatment*	m/z	Assigned sequences	Disulfide bonds	C + IAM	Predicted structures
L349P	*BrCN*	9158.97	(309-345) + (346-384) + (385-391)	315-388 318-382 346-357		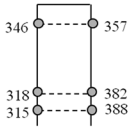
	Trypsin	9236.62	one cleavage with the two peptides still connected	315-388 318-382 346-357		
		6808.94	(309-345) + (346-384) + (385-391)	315-388 318-382 346-357		
	Asp N	2134.98	(343-361)	346-357		
	Glu C	2497.37	(343-361)	346-357		
Δ342-348	*Trypsin*	1719.76	(309-323)	315-318		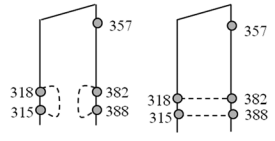
	Asp N	1703.78	(340-Δ-361) + IAM	/	357	
		1931.79	(374-391)	382-388		
	Glu C	2493.05	(309-319) + (380-391)	315-388 318-382		
		2511.02	(309-316) + (317-319) + (380-391)	315-388 318-382		
		1731.82	(338-Δ-359) + IAM	/	357	
		1261.58	(380-391)	382-388		
C315S	*BrCN*	8430.21	(309-345) + (346-384)	318-382 & 346-357		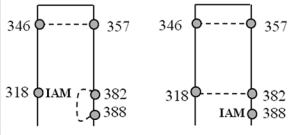
		4963.65	(309-345) + (385-391)	318-388		
	Trypsin	6529.09	(309-345) + (346-384) + (385-391) + IAM	318-382 & 346-357 or 318-388 & 346-357	382 or 388	
		4766.59	(345-348) + (352-391)	346-357 & 382-388		
		1763.88	(309-323) + IAM	/	318	
	Glu C	2512.18	(338-359)	346-357		
		1261.57	(380-391)	382-388		
	BrCN &GluC	1578.70	(346-359)	346-357		
C382G	*BrCN*	4250.39	(309-345)	315-318		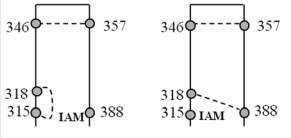
		4151.99	(346-384)	346-357		
	Trypsin	6449.54	(309-323) + (345-348) + (352-391) +IAM	315-388 & 346-357 or 318-388 & 346-357	315 or 318	
		4779.36	(345-348) + (352-391) + IAM	346-357	388	
		1720.41	(309-323)	315-318		
	Glu C	2512.17	(338-359)	346-357		
		2506.12	(309-319) + (380-391) + IAM	315-388 or 318-388	315 or 318	
		1564.71	(317-319) + (380-391)	318-388		

Figure 5. Schematic summary of the enzymatic or chemical processing results of Sap C mutants. Informative MS data derived from each enzymatic or chemical treatment for each mutant are summarized ('*m*/*z*' column). The respective attributions are also reported ('assigned sequences' column) together with the deduced disulfide bridges ('disulfide bonds' column) and the IAM-modified cysteines ('C + IAM' column). The patterns of predicted disulfide bridges occurring in each mutant are depicted in the cartoon on the right. Continuous lines represent the protein, whereas dashed lines indicate the disulfide bonds between cysteine residues (marked as small circles).

incubated, with or without Cath D O/N, and products were separated by sodium dodecyl sulfate–polyacrylamide gel electrophoresis (SDS–PAGE). As shown, WT Sap C band remained unaltered after Cath D treatment, and the L349P mutant showed only partial digestion. In contrast, a substantial decrease of the undigested product was observed for the other mutants, confirming susceptibility to Cath D action (Fig. 8A). Consistently, SDS–PAGE and MS analysis demonstrated that the Δ342-348 mutant was the most sensitive mutant to Cath D treatment, followed by the C382G and C315S proteins, while the L349P mutant exhibited only a slightly increased sensitivity, compared with the WT protein (Fig. 8B). Such differential resistance of disease-associated mutants to protease action is likely to underlie the lower stability revealed by the mutants *in vivo*.

To better assess the role of disulfide bonds in protein stability, all the mutants were also treated with dithiothreitol (DTT) before Cath D digestion. Insulin was used as a control, since it contains both inter- and intramolecular disulfide bridges. While insulin was only partially digested when the disulfide bonds were intact, the protein was completely hydrolysed by Cath D after DTT reduction, indicating that the partial resistance of insulin to Cath D is due to the structure of the protein, tightened by its disulfide bonds. When the same strategy was applied to Sap C, its disulfide bridges turned out to be highly resistant to DTT. DTT concentration (5 mM) able to completely reduce insulin did not break the disulfide bridges of the WT and mutant proteins (Supplementary Material, Fig. S2), except the C382G mutant, one of whose disulfide bonds was reduced. Thus, the solid structure of Sap C makes it impervious even to DTT. To definitively demonstrate that it is the structure of Sap C and not its primary sequence that makes it Cath D resistant, digestions were performed using high DTT concentration (100 mM). As expected, the totally reduced WT and mutant forms of Sap C were

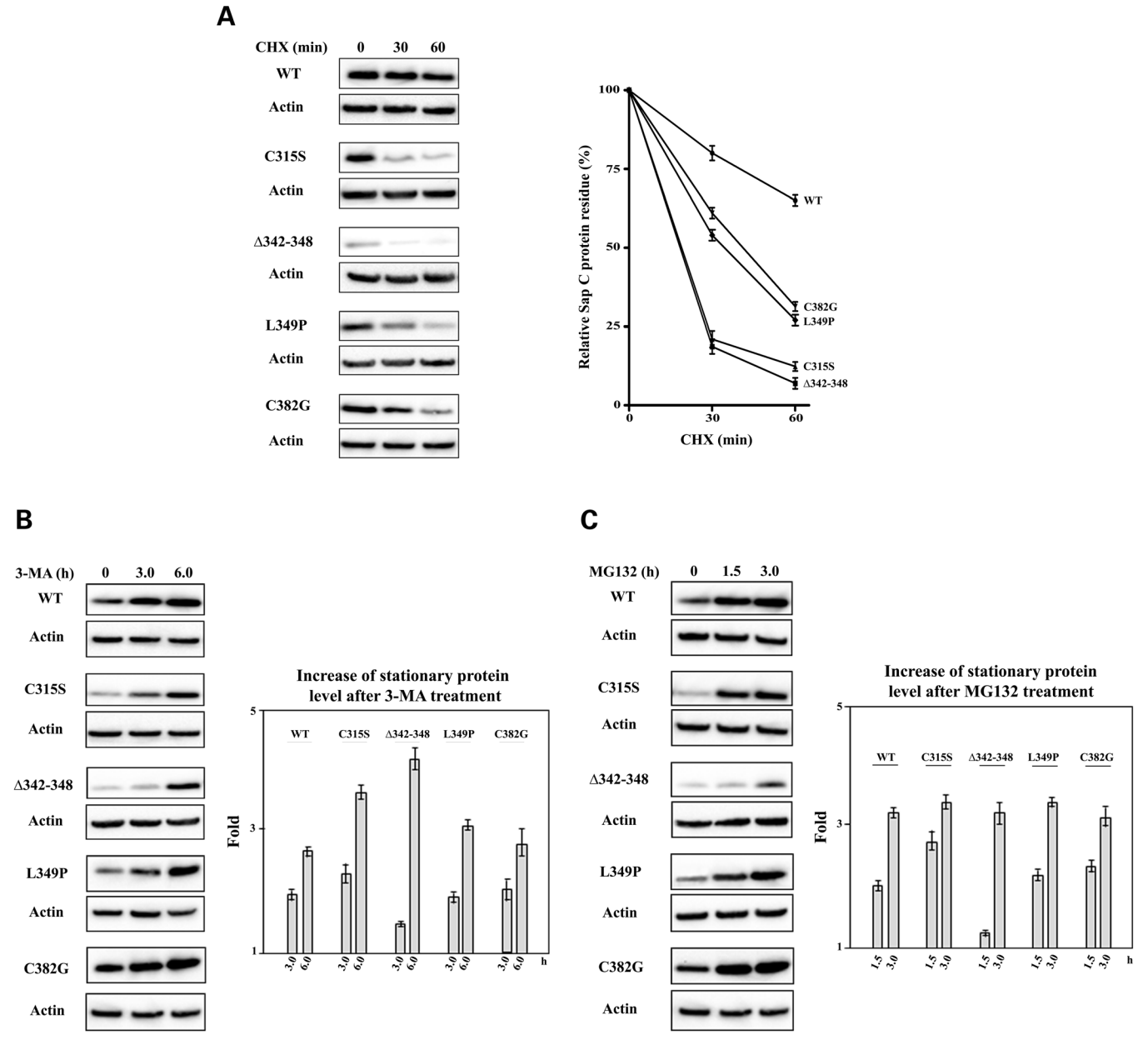

Figure 6. Stability and degradation of WT Sap C and disease-causing mutants. (**A**) Panels show WT and mutant Sap C protein levels in transfected COS-1 cells after CHX treatment for the indicated times. The percentage of relative Sap C protein residue is shown (right). (**B**) Effect of 3-MA and (**C**) MG132 treatments on WT and mutant Sap C protein degradation and relative increase of stationary protein level. Actin level indicates equal loading.

readily digested by Cath D already after a 1 h incubation (O/N digestion in Fig. 9).

DISCUSSION

GD is caused by a deficit of GCase enzyme or, rarely, of its activator Sap C. Here, we structurally, biochemically and functionally characterized four of the five reported Sap C mutations underlying GD. The present study imparts a series of novelties on the mechanism by which mutations affecting the Sap C protein cause the pathology. Similar to what observed for the WT protein, we found that all mutants interact with anionic phospholipid-containing membranes at low pH and activate GCase. These mutants, however, display an altered structure, which make them prone to proteolytic degradation by lysosomal enzymes. The produced data document that their instability is due to structural rearrangements resulting from aberrantly formed intramolecular disulfide bonds. While the p.C382F Sap C mutant was not considered in this study, based on the overall relatively homogeneous biochemical behavior of mutants with an affected cysteine residue and the similar clinical features of the two patients heterozygous for the p.C382G and p.C382F changes, we expect a comparable structural perturbation and

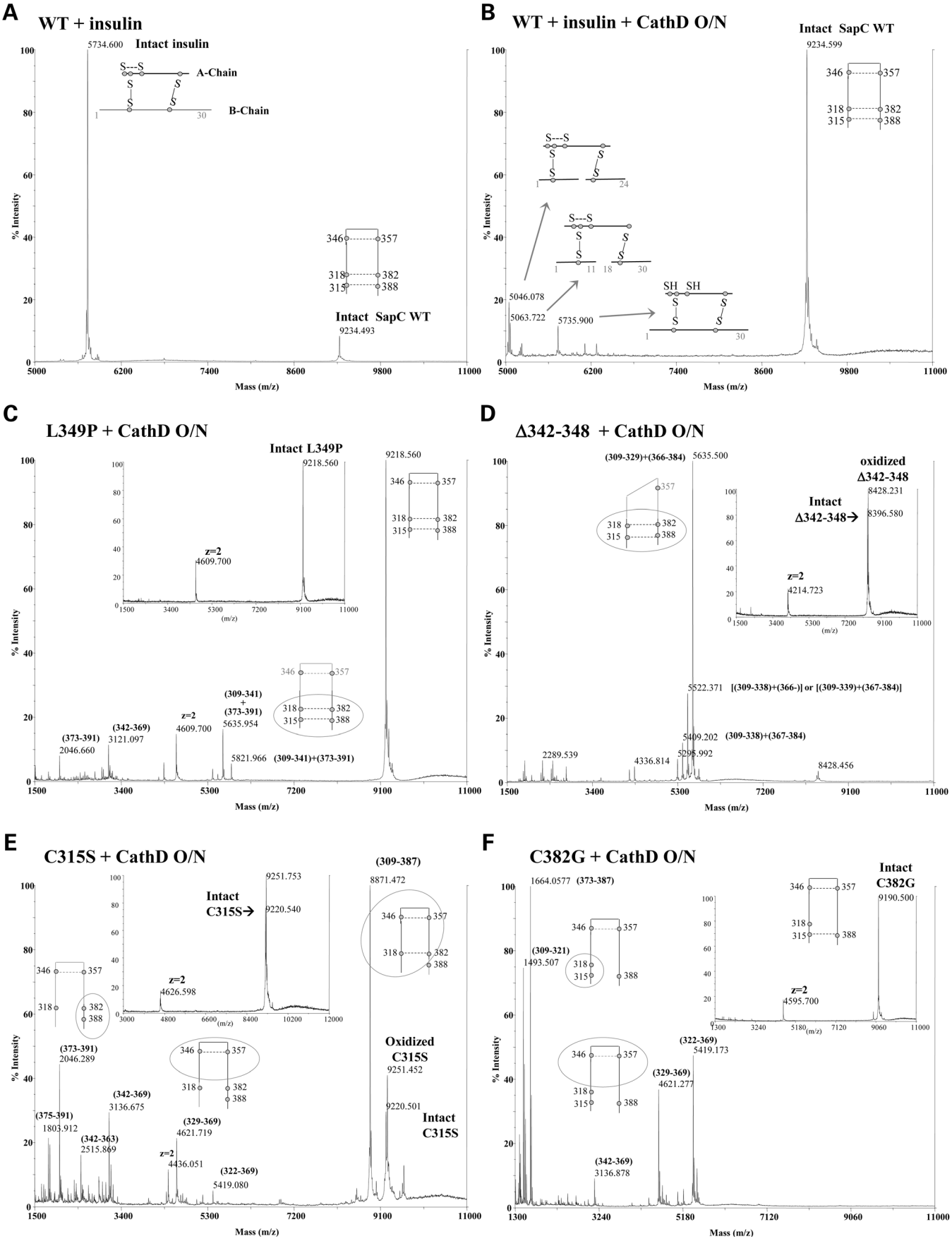

accelerated degradation also for the Sap C mutant carrying the p.C382F substitution.

Disulfide bonds in proteins play an important role in the folding process and in stabilizing the three-dimensional structure of the molecule (21). By characterizing the assembly of the disulfide bridges in the C315S, Δ342-348, L349P and C382G mutants, we documented that their rearrangement makes the mutants more accessible to the attack of proteolytic enzymes.

In silico analysis (YASPIN—http://www.ibi.vu.nl/programs/yaspinwww) (22) of Sap C structure revealed that the protein has two principal structures, α-helices and coils, which are distributed along the molecule in an alternate fashion (Supplementary Material, Fig. S3). As reported by Liu *et al.* (23), the *N*-terminal half of the protein bears a number of positive charges that have been considered responsible for lipid binding, while it holds a few negative charges and some hydrophilic residues at the *C*-terminus. In the L349P mutant, the replacement of Leu^{349} by proline was predicted to have an effect on structure flexibility (24); this substitution occurs in an unstructured region, and we did not observed any substantial rearrangement of the disulfide bonds. Further studies are required to understand the impact of the amino acid change on protein structure. In the Δ342-348 mutant, the structural rearrangement due to the loss of Cys^{346} (Supplementary Material, Fig. S3), and reduced positive charge due to loss of Lys^{344} and Lys^{348} would have been expected to result in a lower lipid-binding ability. On the contrary, our results show that the interaction with lipid membranes of Δ342-348 variant was comparable with the WT protein. This might be explained by the observation of Liu *et al.* (23), indicating that the helices α1, containing two lysine residues (Lys^{323} and Lys^{327}) and α5 of Sap C significantly contribute in the membrane anchoring process. Besides, with the native 315–388 and 318–382 disulfide bonds partially missing, the mutant was predicted to assume different structures due to disulfide bridge rearrangements (Fig. 5). One of them (the one bearing 315–318 and 382–388 disulfide bridges) is probably much more flexible and linear, exposing large portions of itself to proteolytic enzymes.

According to YASPIN's predictions, substitution of Cys^{315} by serine or Cys^{382} by glycine generates no changes in the local α-helix. Therefore, in these mutants, the absence of one or both of the synergistic disulfide bonds connecting the extremes of the protein appears to be crucial in determining different conformations and the observed biochemical effects.

The residues mutated in three pathological variants are strictly conserved in Sap C orthologs. Based on the data here reported, we consider that, as many recessive diseases, caused by two inactivating hits, Sap C deficiency pathogenicity, is strictly linked to occurrence of a perturbed protein fold, resulting in faster protein degradation that would trigger system failure. Moreover, the findings also increase the basic understanding of the nature of the primary biochemical abnormality with different Sap C mutations and help to define a possible mechanism to explain the substantial phenotypic heterogeneity that characterize this variant GD disease. Accuracy in protein folding is a crucial aspect for Sap C proper maintenance of cellular functionality.

MATERIALS AND METHODS

Construction of Sap C mutant prokaryotic expression vectors

Plasmids coding mutant Sap C proteins carrying the C315S, L349P or C382G amino acid substitutions were generated by site-directed mutagenesis (Stratagene, La Jolla, CA, USA) using the pPAL7-spacer-Sap C vector (17) as template and the following primer pairs: SapC_C315S Fw 5′-G ACT TCT TCT GAT GTT TAC T**C**T GAG GTG TGT GAA TTC CTG G-3′ and Rv 5′-C CAG GAA TTC ACA CAC CTC A**G**A GTA AAC ATC AGA AGA AGT C-3′; SapC_L349P Fw 5′-C AAA ATG TGC TCG AAG C**C**G CCG AAG TCC CTG TCG G-3′ and Rv 5′-C CGA CAG GGA CTT CGG C**G**G CTT CGA GCA CAT TTT G-3′; SapC_C382G Fw 5′-GTC AGC CCT GAG CTG GTG **G**GC AGC ATG CTG CAC CTC TGC-3′ and Rv 5′-GCA GAG GTG CAG CAT GCT GC**C** CAC CAG CTC AGG GCT GAC-3′. The Sap C mutant carrying the Δ342-348 deletion was created by overlap extension PCR (25). Briefly, two PCR products representing the flanking regions of the DNA sequence to be deleted were prepared using the following primer pairs: *Hind*III-SapC Fw 5′-TG ACT TCT TCT GAT GTT TAC TGT GAG GTG-3′, SapC_Δ342-348 Rv 5′-CTT CGG CAG AGC GTC GAG TAT TTC-3 and SapC Δ342-348 Fw 5′-CTC GAC GCT CTG CCG AAG TCC-3′, *Xho*I-SapC Rv 5′-TTA CGT GCC AGA GCA GAG GTG CAG-3′ (the encompassing the deleted region). In the next step, the two PCR products were used as template for a ligation PCR containing the outermost primer pair (*Hind*III-SapC Fw and *Xho*I-SapC Rv). Finally, the amplified fragment was cloned into the Profinity eXact pPAL7 expression vector (Bio-Rad Laboratories, Hercules, CA, USA). The identities of all constructs were verified by bidirectional sequencing (ABI BigDye terminator Sequencing Kit v3.1 and ABI Prism 3500 Genetic Analyzer, Applied Biosystems, Foster City, CA, USA).

Construction of WT and mutant Sap C eukaryotic expression vectors

The cDNA coding for the Sap C sequence was generated from pPAL7-spacer-Sap C (17) by PCR using the specific primers *Nhe*I-SapC Fw 5′-GCT AGC ATG TCT GAT GTT TAC TGT GAG-3′ and *Xho*I-SapC Rv 5′-CTC GAG CGT GCC AGA GCA GAG GTG CAG-3′. The amplified product was digested with *Nhe*I and *Xho*I and cloned into the pcDNA6/V5-HisA eukaryotic expression vector (Invitrogen, Carlsbad, CA, USA).

Figure 7. Sensitivity of WT Sap C and disease-causing mutants to Cath D protease activity. (**A**) Spectrum of untreated WT Sap C and insulin showing the measured molecular weights of the intact proteins. (**B**) The same two proteins after O/N incubation with Cath D. WT Sap C remained intact, while the peak corresponding to undigested insulin decreased markedly and lower-molecular-weight digestion products appeared, indicating protein digestion. (**C**–**F**) Spectra of the reactions performed on each of the disease-causing Sap C mutants. Mass spectra of O/N Cath D digestions are shown. The numbers in parentheses indicate the peptides corresponding to the observed ions. Ellipses highlight the regions from which the fragments detected by MS derive; insets show the spectra of the proteins before the incubation with Cath D. The added schemes represent the protein configuration corresponding to the nearest peaks.

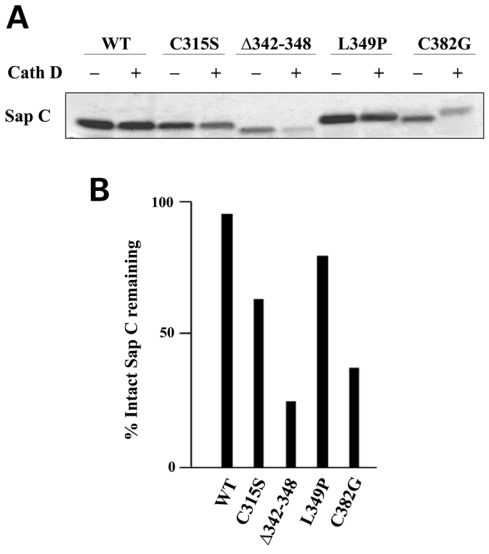

Figure 8. Cath D digestion of WT Sap C and disease-causing mutants. (**A**) WT Sap C and mutants were incubated in the absence and presence of Cath D (O/N, 37°C), analyzed by SDS–PAGE and visualized by silver staining. (**B**) The amount of undigested WT Sap C and mutant was quantified as the percentage of original level.

Mutant Sap C coding sequences (C315S, Δ342-348, L349P and C382G) were created by PCR using the appropriate pPAL7-spacer-Sap C construct as template and the primer pair *Nhe*I-SapC_C315S Fw 5′GCT AGC ATG TCT GAT GTT TAC T**C**T GAG-3′ and *Xho*I-SapC Rv or *Nhe*I-SapC Fw and *Xho*I-SapC Rv. PCR products were cloned in the pcDNA6/V5-HisA vector and sequence identity of WT and mutant Sap C constructs was confirmed by sequencing.

Expression and purification of the recombinant Sap C proteins

Recombinant Sap C proteins were expressed in *E. coli* Origami 2 (DE3) competent cells (Novagen, Germany) and purified following the previously described protocol (17). Amount, purity and integrity of the produced proteins were evaluated using the bicinchoninic acid assay (Pierce, Rockford, IL, USA) (26) and silver staining (SilverQuest^{TM} Staining Kit, Invitrogen).

Cell culture, transfection and inhibitor treatments

COS-1 cells (American Type Culture Collection, Manassas, VA, USA) were cultured in DMEM supplemented with 10% heat-inactivated FBS, 2 mM glutamine, 100 units/ml of penicillin and 100 μg/ml of streptomycin and maintained at 37°C in a humidified atmosphere containing 5% CO_2.

Subconfluent cells were transfected using the Fugene6 transfection reagent (Roche Diagnostics, Mannheim, Germany) according to the manufacturer's instruction. Cells were treated with CHX (10 μg/ml), 3-MA (3 mM) or MG132 (25 μM) (Sigma–Aldrich, St Louis, MO, USA).

Western blot analysis

Cells were lysed in radioimmunoprecipitation assay buffer, pH 8.0, containing 20 mM NaF, 1 mM Na_3VO_4 and protease inhibitors. Lysates were kept on ice (30 min), and then centrifuged at 16 000*g* (20 min, 4°C). Supernatants were resolved by SDS–PAGE and transferred to polyvinylidene difluoride membranes (Bio-Rad Laboratories). Blots were blocked for 1 h with 5% non-fat milk powder in phosphate-buffered saline (PBS) containing 0.1% Tween-20 and incubated for 1 h with specific antibodies. Primary and secondary antibodies were diluted in blocking solution. Immunoreactive proteins were detected by an ECL Advance^{TM} Western Blotting Detection Kit, according to the manufacturer's instructions (GE Healthcare, Buckinghamshire, UK).

Mass spectrometry analysis

Protein samples were spotted onto a MALDI plate using the dried droplet technique and a matrix [30 mg/ml 2,5-dihydroxybenzoic acid (Sigma–Aldrich) in 50% acetonitrile, 1% phosphoric acid]. All the analyses were performed using a Voyager-DE STR (Applied Biosystems, Framingham, MA, USA) operated in the reflector mode, using delayed extraction mode (delay time 750 ns), 25 000 V accelerating voltage and 66% grid. Spectra were acquired in the 1000–25 000 *m*/*z* range. The spectra were internally calibrated and processed via the Data Explorer software (Applied Biosystems).

Chemical and enzymatic treatments

Alkylation was performed by incubating the proteins with IAM in a 10-fold molar excess respect to the cysteines present in the sample (37°C, 1 h). BrCN treatments were carried out by incubating recombinant WT or mutant Sap C in 50 mg/ml BrCN in 70% trifluoracetic acid (O/N in the dark at room temperature). Excess of BrCN was removed by adding acetonitrile twice and drying the solution in a SpeedVac concentrator (Thermo Scientific, Waltham, MA, USA). Enzymatic digestions were performed using trypsin (Promega, Madison, WI, USA), Glu C or Asp N (Roche Diagnostics, Basel, Switzerland) in enzyme–protein (w/w) ratios of 1:50 in 50 mM ammonium bicarbonate (O/N at 37°C). Cath D (Sigma–Aldrich) treatment was performed in 10 mM sodium acetate, pH 4.5, in a Sap C/Cath D ratio of 1:50 at 37°C.

DTT treatments of insulin (Sigma–Aldrich) or recombinant WT or mutant Sap C proteins were realized by incubating the proteins for 1 h at 56°C in the presence of 5 or 100 mM DTT, corresponding to a 100 or >1000 M excess, respectively, relative to the cysteines present in the solution.

Liposome preparation

LUVs, composed of either phosphatidylcholine (PC) and phosphatidylserine (PS) (Avanti Polar Lipids, Alabaster, AL, USA) in molar ratio of 80:20 or PC, PS and GC in molar ratio of 75:20:5, were prepared as previously reported (19). Briefly, appropriate amounts of lipids dissolved in chloroform–methanol 2:1 (v/v) were mixed and the solvent was evaporated under nitrogen. The resulting lipid films were dried O/N in vacuum

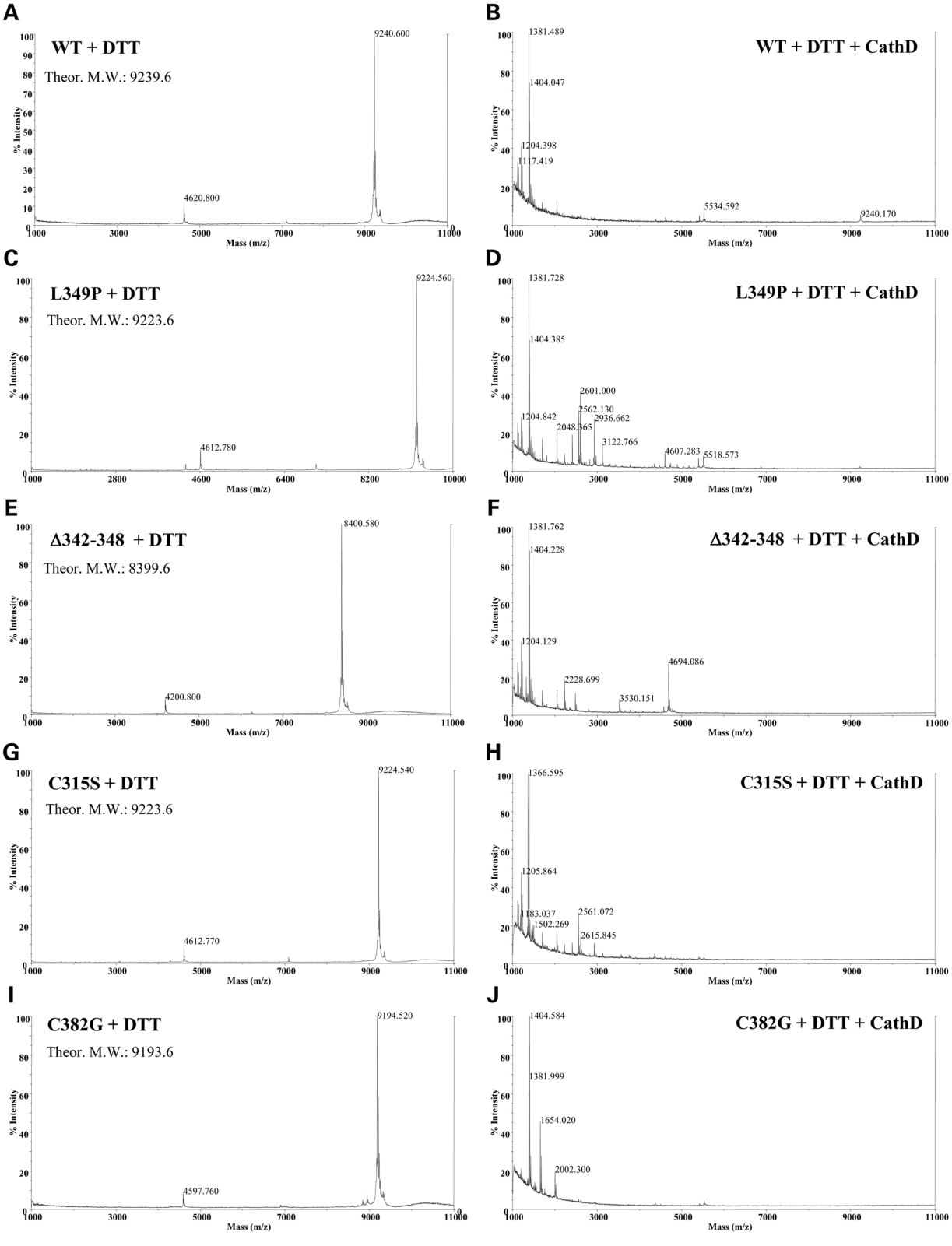

Figure 9. Cath D digestion of WT Sap C and disease-causing mutants after complete reduction. (**A**, **C**, **E**, **G** and **I**) WT and mutant Sap C proteins were treated with high-concentration of DTT (100 mM); each panel displays the theoretical molecular weight (theor. M.W.) of each protein, with all cysteines in the reduced state. *m*/*z* values correspond to completely reduced (and protonated) proteins. (**B**, **D**, **F**, **H** and **J**) Spectra acquired after O/N Cath D digestion of the reduced proteins. Peaks corresponding to the intact proteins disappeared, while lower-MW products appeared, indicating complete digestion of each mutant.

desiccator. The dry lipids were dispersed by vortex mixing in 2 mM L-histidine, 2 mM *N*-Tris hydroxymethyl methyl-2-aminoethane sulfonic acid, 150 mM NaCl, 1 mM EDTA, pH 7.4, followed by 10 cycles of freeze–thawing. Finally, they were passed 21 times through two stacked 0.1 μm diameter pore polycarbonate membranes (Nucleopore Corp., Pleasanton, CA, USA) in a Liposofast-Miniextruder (Avestin, Ottawa, ON, Canada).

Surface plasmon resonance spectroscopy

Real-time lipid–protein interaction analysis was performed at 25°C in a Biacore X instrument (Biacore International AB, Uppsala, Sweden) on an L1 sensor chip (GE Healthcare). For immobilization of liposomes, 60 μl of a liposome solution (0.5 mM in 2 mM L-histidine, 2 mM *N*-Tris hydroxymethyl methyl-2-aminoethane sulfonic acid, 150 mM NaCl, 1 mM EDTA, pH 7.4) were injected at a flow rate of 5 μl/min. Unbound liposomes were removed by washing with 10 μl of 25 mM sodium hydroxide at the flow rate of 30 μl/min. To obtain complete saturation of the surface, 40 μl of the liposome solution was newly injected, and the surface was washed with 10 μl of 25 mM sodium hydroxide at a flow rate of 30 μl/min to remove multilamellar vesicles and to stabilize the baseline, as recommended by the manufacturer's instructions (Biacore International). After immobilization of liposomes, a signal increase of 6000–7000 response units was achieved. For measurement of the interaction of the protein with the immobilized liposomes, the surface was washed with running buffer (10 mM sodium acetate, 150 mM NaCl, 1 mM EDTA, pH 5.0 or 10 mM *N*-2-hydroxyethylpiperizine-*N*-2-ethanesulphonic acid, 150 mM NaCl, 1 mM EDTA, pH 7.0), and the signal was adjusted to zero. Sap C WT and mutants in running buffer were injected with a flow rate of 30 μl/min for 120 s followed by injection of running buffer. All measurements were repeated at least three times.

GCase assays

GCase activity was measured utilizing anionic phospholipid-containing LUVs, recombinant Sap C proteins as activators and either 4-MU-Glc (Sigma–Aldrich) or [^{3}H]GC as substrate. In the first case, the assay was performed in a final volume of 0.2 ml containing 10 mM sodium acetate, 150 mM NaCl, 1 mM EDTA, pH 5.0, 1% (w/v) BSA, 2.5 mM 4-MU-Glc, 4 ng of GCase purified from human placenta, 100 μg of PC:PS-containing LUVs and different amounts of Sap C. Assay mixtures were incubated for 30 min at 37°C. GCase activity was measured fluorimetrically (18). In the second case, the assay was performed in a final volume of 0.2 ml containing the same buffer described above, 1% (w/v) BSA, 4 ng of GCase purified from human placenta, 200 μg of PC:GC-containing LUVs and different amounts of Sap C. The GC included in the liposomes was supplemented with the radiolabeled compound ([^{3}H]GC) to a specific activity of 2500 dpm/nmol. Assay mixtures were incubated for 30 min at 37°C. The enzymatically released [^{3}H]glucose was measured as previously described (27).

Proteolysis of WT and mutants Sap C by Cath D

Purified recombinant proteins were treated with Cath D (Sigma–Aldrich). A ratio 1:50 (w/w) of Cath D to protein in 10 mM sodium acetate, pH 4.5, was incubated O/N at 37°C. Then, the reaction mixtures were subjected to SDS–PAGE and stained with silver. The band densities of intact Sap C were quantified in digested and undigested proteins using Alpha View SA (Protein Simple, Santa Clara, CA, USA).

Confocal laser scanning microscopy

COS-1 cells (30×10^3) were seeded on glass coverslips, transfected with the various constructs for 24 h, fixed with 3% paraformaldehyde for 30 min at 4°C and permeabilized with 0.5% Triton X-100 for 10 min at room temperature.

For double immunostaining, the cells were incubated with a specific mouse monoclonal primary antibody (anti-V5, R960-25, Invitrogen) for 1 h at room temperature, rinsed twice with PBS and incubated with the secondary anti-mouse antibody conjugated with Alexa Fluor 488 (Molecular Probes, Eugene, OR, USA) for 1 h at room temperature. Cells were then rinsed three times with PBS, incubated 1 h with a specific goat polyclonal primary antibody (anti-Cath D, sc-6487, Santa Cruz Biotechnology, Dallas, TX, USA), rinsed twice with PBS and incubated 1 h with the secondary anti-goat antibody conjugated with Alexa Fluor 555 (Molecular Probes).

Finally, glass coverslips were mounted on microscope slides using the Vectashield antifade medium containing DAPI (Vector Laboratories, Burlingame, CA, USA) and analyzed by a Leica TCS SP2 AOBS apparatus, utilizing excitation spectral laser lines at 405, 488 and 555 nm, tuned with an acousto-optical tunable filter. Image acquisition and processing were conducted using the Leica Confocal Software 2.3 (Leica Lasertechnik, Heidelberg, Germany) and Adobe Photoshop 7.0 (Adobe Systems Incorporated, San Jose, CA, USA). Signals from different fluorescent probes were taken in sequential scanning mode.

SUPPLEMENTARY MATERIAL

Supplementary Material is available at *HMG* online.

ACKNOWLEDGEMENTS

We thank M. Signore (Istituto Superiore di Sanità, Roma, Italy) for his help in image acquisition at confocal scanning laser microscopy.

Conflict of Interest statement. None declared.

FUNDING

This work was supported, in part, by ISS Ricerca Corrente 2013.

REFERENCES

1. Beutler, E. and Grabowski, G.A. (2001) Gaucher disease. In Scriver, C.R., Beaudet, A.L., Sly, W.S., Valle, D., Childs, B., Kinzler, K.W. and Volgstein, B. (eds), *The Metabolic & Molecular Bases of Inherited Disease*, 8th edn. McGraw-Hill, New York, Vol. III. pp. 3635–3668.

2. O'Brien, J. and Kishimoto, Y. (1991) Saposin proteins: structure, function, and role in human lysosomal storage disorders. *FASEB J.*, **5**, 301–308.
3. Vaccaro, A.M., Salvioli, R., Tatti, M. and Ciaffoni, F. (1999) Saposins and their interaction with lipids. *Neurochem. Res.*, **24**, 307–314.
4. Wrobe, D., Henseler, M., Huettler, S., Pascual Pascual, S.I., Chabas, A. and Sandhoff, K. (2000) A non-glycosylated and functionally deficient mutant (N215H) of the sphingolipd activator protein B (Sap-B) in a novel case of metachromatic leukodystrophy (MLD). *J. Inherit. Metab. Dis.*, **23**, 63–76.
5. Spiegel, R., Bach, G., Sury, V., Mengistu, G., Meidan, B., Shaley, S., Shneor, Y., Mandel, H. and Zeigler, M. (2005) A mutation in the saposin A coding region of the prosaposin gene in an infant presenting as Krabbe disease: first report of saposin A deficiency in humans. *Mol. Genet. Metab.*, **84**, 160–166.
6. Vaccaro, A.M., Salvioli, R., Barca, A., Tatti, M., Ciaffoni, F., Maras, B., Siciliano, R., Zappacosta, F., Amoresano, A. and Pucci, P. (1995) Structural analysis of Saposin C and B. *J. Biol. Chem.*, **270**, 9953–9960.
7. de Alba, E., Weiler, S. and Tjandra, N. (2003) Solution structure of human saposin C: pH-dependent interaction with phospholipid vesicles. *Biochemistry*, **42**, 14729–14740.
8. Christomanou, H., Aignesberger, A. and Linke, R.P. (1986) Immunochemical characterization of two activator proteins stimulating enzymic sphingomyelin degradation in vitro. Absence of one of them in a human Gaucher disease variant. *Biol. Chem. Hoppe Seyler*, **367**, 879–890.
9. Christomanou, H., Chabas, A., Pampols, T. and Guardiola, A. (1989) Activator protein deficient Gaucher's disease. *Klin. Wochenschr.*, **67**, 999–1003.
10. Tylki-Szymanska, A., Czartoryska, B., Vanier, M.T., Poorthuis, B.J., Groener, J.A., Lugowska, A., Millat, G., Vaccaro, A.M. and Jurkiewicz, E. (2007) Non-neuronopathic Gaucher disease due to saposin C deficiency. *Clin. Genet.*, **72**, 538–542.
11. Amsallem, D., Rodriguez, D., Vanier, M.T., Khayat, N., Millat, G., Campello, M., Guillame, C. and Billette De Villemeur, T. (2005) Third case of Gaucher disease with sap-C deficiency and evaluation of twelve months' therapy by miglustat. *J. Inherit. Metab. Dis.*, **28**(Suppl. 1), 152.
12. Vanier, M.T. and Millat, G. (2009) Are sphingolipid activator deficiencies underdiagnosed? *Int. J. Clin. Pharmacol. Therap.*, **47**(Suppl. 1), S147–S148.
13. Schnabel, D., Schroder, M. and Sandhoff, K. (1991) Mutation in the sphingolipid activator protein 2 in a patient with a variant of Gaucher disease. *FEBS Lett.*, **284**, 57–59.
14. Rafi, M.A., de Gala, G., Zhang, X.L. and Wenger, D.A. (1993) Mutational analysis in a patient with a variant form of Gaucher disease caused by Sap-2 deficiency. *Somat. Cell. Mol. Genet.*, **19**, 1–7.
15. Diaz-Font, A., Cormand, B., Santamaria, R., Vilageliu, L., Grinberg, D. and Chabas, A. (2005) A mutation within the saposin D domain in a Gaucher disease patient with normal glucocerebrosidase activity. *Hum. Genet.*, **117**, 275–277.
16. Vaccaro, A.M., Motta, M., Tatti, M., Scarpa, S., Masuelli, L., Bhat, M., Vanier, M.T., Tylki-Szymanska, A. and Salvioli, R. (2010) Saposin C mutations in Gaucher disease patients resulting in lysosomal lipid accumulation, saposin C deficiency, but normal prosaposin processing and sorting. *Hum. Mol. Genet.*, **19**, 2987–2997.
17. Motta, M., Tatti, M., Martinelli, S., Camerini, S., Scarpa, S., Crescenzi, M., Tartaglia, M. and Salvioli, R. (2011) Efficient one-step chromatographic purification and functional characterization of recombinant human Saposin C. *Protein Expr. Purif.*, **78**, 209–215.
18. Vaccaro, A.M., Tatti, M., Ciaffoni, F., Salvioli, R. and Roncaioli, P. (1992) Reconstitution of glucosylceramidase on binding to acidic phospholipid-containing vesicles. *Biochim. Biophys. Acta*, **1119**, 239–246.
19. Vaccaro, A.M., Tatti, M., Ciaffoni, F., Salvioli, R., Barca, A. and Scerch, C. (1997) Effect of saposins A and C on the enzymatic hydrolysis of liposomal glucosylceramide. *J. Biol. Chem.*, **272**, 16862–16867.
20. Liou, B., Kazimierczuk, A., Zhang, M., Scott, C.R., Hedge, R.S. and Grabowski, G.A. (2006) Analyses of variant acid β-glucosidases. *J. Biol. Chem.*, **281**, 4242–4253.
21. Takase, K., Higashi, T. and Omura, T. (2002) Aggregate formation and the structure of the aggregates of disulfide-reduced proteins. *J. Protein Chem.*, **21**, 427–433.
22. Lin, K., Simossis, V.A., Taylor, W.R. and Heringa, J. (2005) A simple and fast secondary structure prediction method using hidden neural networks. *Bioinformatics*, **21**, 152–159.
23. Liu, A., Wenzel, N. and Qi, X. (2005) Role of lysine residues in membrane anchoring of saposin C. *Arch. Biochem. Biophys.*, **443**, 101–112.
24. Bett, M.J. and Russell, R.B. (2003) Amino acid properties and consequences of substitutions. In Barnes, M.R. and Gray, I.C. (eds)., *Bioinformatics for Geneticists*, Wiley, J. & Sons, Ltd, USA. pp. 289–316.
25. Lee, J., Lee, H.J., Shin, M.K. and Ryu, W.S. (2004) Versatile PCR-mediated insertion or deletion mutagenesis. *Biotechniques*, **36**, 398–400.
26. Smith, P.K., Krohn, R.I., Hermanson, G.T., Mallia, A.K., Gartner, F.H., Provenzano, M.D., Fujimoto, E.K., Goeke, N.M., Olson, B.J. and Klenk, D.C. (1985) Measurement of protein using bicinchoninic acid. *Anal. Biochem.*, **150**, 76–85.
27. Suzuki, K. (1987) Enzymatic diagnosis of sphingolipidoses. *Methods Enzymol.*, **138**, 727–762.